

Direct dynamics simulations of photoexcited charge-transfer-to-solvent states of the $\text{I}^-(\text{H}_2\text{O})_6$ cluster

Toshiyuki Takayanagi*, Kenta Takahashi

Department of Chemistry, Saitama University, 255 Shimo-Okubo, Sakura-ku, Saitama City, Saitama 338-8570, Japan

Abstract

Direct molecular dynamics simulations have been carried out to understand the relaxation dynamics of photoexcited charge-transfer-to-solvent (CTTS) states for the $\text{I}^-(\text{H}_2\text{O})_6$ cluster and the subsequent excess electron stabilization dynamics by solvent molecules. Due to a small singlet-triplet splitting, the lowest triplet potential energy surface at the B3LYP-level calculations was used to model the CTTS singlet excited-state surface. Two book-type structures, which correspond to the lowest ground-state minimum-energy geometries, were vertically excited with the initial kinetic energy being zero. Although these two structures have a very similar geometry, it was found that the excess electron localization dynamics was totally different.

Corresponding author. *E-mail address*: tako@chem.saitama-u.ac.jp (T. Takayanagi)

1. Introduction

Iodide anion-water clusters are known to be good systems for understanding the dynamics of excess electron stabilization by water molecules since electronically excited states of these clusters are precursors of so-called charge-transfer-to-solvent (CTTS) states [1]. It is established that, upon photoexcitation, electron transfer occurs from a Γ valence p -orbital to a very diffuse orbital corresponding to a dipole field formed collectively by polar solvent molecules. Using these photoexcitation processes, Neumark and co-workers [2-6] have applied pump-probe femtosecond laser spectroscopic techniques to the $\Gamma(\text{H}_2\text{O})_n$ cluster anion system and their deuterated analogs and reported the time evolution of excess electron binding energies, which gives detailed information on dynamics of the excess electron stabilization by water molecules. For the $\Gamma(\text{H}_2\text{O})_4$ cluster, the electron binding energy was found to remain constant with simple population decay of the excited state. On the other hand, for larger clusters with $n \geq 5$, a clear increase in electron binding energy was observed after several hundred femtoseconds. This behavior was interpreted as evidence for solvent rearrangement resulting in stabilization of the excess electron in a state localized on the water cluster. This model also accounts for the observed isotope effects showing a slight difference in the time dependence of the excess electron binding energy between $\Gamma(\text{H}_2\text{O})_n$ and $\Gamma(\text{D}_2\text{O})_n$ clusters.

On the theoretical side, Chen and Sheu [7,8] proposed a different interpretation for the femtosecond experiments of Neumark and co-workers [2-4] on the basis of "static" quantum-chemical calculations. Their calculations showed that the presence of the neutral iodine atom significantly destabilizes the excited excess electron in the cluster. They have then concluded that the time-dependent binding energy shifts were due to neutral iodine atom detachment from the water cluster anion rather than to solvent rearrangement. A similar theoretical interpretation was also reported by Kim and co-workers [9] based on static ab initio electronic structure calculations. They have concluded that the iodine atom is readily charge-neutralized upon photoexcitation and released from the cluster, followed by the solvent rearrangement process. Very recently, direct trajectory calculations have been performed to simulate the pump-probe femtosecond experiments. Timerghazin and

Peslherbe [10] and Kolaski et al. [11] have independently carried out direct dynamics simulations on the excited-state potential energy surface using the complete-active-space self-consistent (CASSCF) approach but for a small $\Gamma(\text{H}_2\text{O})_3$ cluster anion. These two groups have suggested that the relaxation of photoexcited $\Gamma(\text{H}_2\text{O})_3$ cluster is a complex process, where both the role of iodine and solvent motions must be included if an accurate picture is to be achieved. However, notice that the ground-state minimum structure of the $\Gamma(\text{H}_2\text{O})_3$ cluster is reported to be somewhat different from the structures of the $\Gamma(\text{H}_2\text{O})_5$ and $\Gamma(\text{H}_2\text{O})_6$ clusters in the ground state. Thus, it is still unknown that the conclusions obtained from the simulation of the $\Gamma(\text{H}_2\text{O})_3$ cluster dynamics may be applicable to the larger cluster dynamics.

Motivated by these considerations as mentioned above, in this letter we report results of direct dynamics simulations of the photoexcitation process of the $\Gamma(\text{H}_2\text{O})_6$ cluster. In order to perform the dynamics simulations on singlet CTTS excited state potential energy surfaces, one has to employ, in principle, the electronic structure method that can properly describe excited-state potential energy surfaces. The use of a multiconfigurational approach such as CASSCF, or multi-reference configuration interaction (MRCI) would be desirable; however, this approach is computationally prohibitive especially for large chemical systems. Instead, we use the lowest triplet potential energy surface at the B3LYP density-functional level [12] to model the lowest singlet CTTS potential energy surfaces [13]. As will be shown later, features of the lowest triplet potential surface are very similar to those of the lowest CTTS singlet excited-state surfaces due to a small singlet-triplet splitting.

2. Computational method

The direct dynamics trajectory calculations were carried out at the hybrid density-functional UB3LYP level [12], which was determined by compromise of computational costs and accuracy. A similar approach was previously employed to simulate the photoexcitation dynamics of the $\Gamma(\text{CH}_3\text{CN})_n^-$ ($n = 2$ and 3) cluster [13]. We employed the BOMD (Born-Oppenheimer molecular dynamics) method implemented in the Gaussian 03 program package [14]. This method uses a fifth-order polynomial fitted to the energy,

gradient, and Hessian at each time step, and then the step size can be taken to be much larger than the step size used in the normal method utilizing only the gradient information. The basis sets used in the BOMD calculations were chosen to be small to save computational time. For an iodine atom, a Stuttgart-Dresden-Bonn quasi-relativistic ECP46MWB effective core potential [15] was employed, but additional diffuse and polarization functions were not augmented. In the case of H₂O molecules, we used the strategy of recent work of Herbert and Head-Gordon [16,17] who have carried out systematic calculations of electron detachment energies for water cluster anions. We employed the 6-31(1+,3+)G* basis sets, where two additional diffuse *s*-orbitals are added on hydrogen atoms while the standard 6-31+G* basis set is used for the O atom. The exponents are scaled values of the outermost *s*-shell of the 6-31+G* basis set of hydrogen with a progression factor being 1/3. In their more recent publication [17], the progression factor of 1/3.32 has been proposed but we have confirmed that these two basis sets give very similar results.

We have carried out 1500-fs direct dynamics simulations. The initial structures having the ground-state geometries of I⁻(H₂O)₆ were vertically excited. We set the initial kinetic energies of the system to zero. The structures of the I⁻(H₂O)_{*n*} clusters have been extensively studied in the past [18]. It is now established that the geometric structures of the ground-state I⁻(H₂O)_{*n*} clusters are governed by a combination of the interaction between I⁻ and the dipole moment of water network and the hydrogen-bond interactions between I⁻ and the dangling hydrogen atoms. According to the theoretical work of Lee and Kim [18], the I⁻(H₂O)₆ cluster anion has several low-energy conformers. They have shown that the two book-type conformers are nearly isoenergetic and more stable than other conformers. These two structures are denoted as Bd and Bf in the paper of Lee and Kim [18] (see *t* = 0 structures in Figs. 3 and 5 below) and we will use the same notation hereafter. Both the Bd and Bf structures have seven water-water hydrogen bonds. The I⁻ anion is supported by four hydrogen-bonds by dangling hydrogen atoms. The structural difference between Bd and Bf is seen in the site of a remaining one dangling hydrogen atom. In the Bd structure, it is seen that the remaining dangling hydrogen atom is away from the I⁻ anion, while, in the Bf structure, the remaining dangling hydrogen atom is close to the I⁻ anion. The present B3LYP/6-31(1+,3+)G* level calculations show that the Bd structure is more stable than the

Bf structure by 1.6 kcal/mol without zero-point energy correction. We have employed these two conformers as the initial geometries of photoexcitation.

It should be important to demonstrate the feasibility to use the triplet B3LYP potential energy surface as a model of the singlet CTTS excited-state surface before presenting results of molecular dynamics calculations. Fig. 1 compares the potential energy curves for the $\Gamma(\text{H}_2\text{O})_4$ cluster for which complete-active-space second-order perturbation (CASPT2) results [19] are available. The ground-state $\Gamma(\text{H}_2\text{O})_4$ cluster in the most stable form is known to have the cyclic structure with C_4 symmetry, as shown in Fig. 1. The potential energy curves are plotted as a function of the dihedral angle between the "crown" H atoms and the plane of the oxygen atoms. For each choice of the scanned dihedral angle, the remaining degrees of freedom were optimized for the ground state, while retaining C_4 symmetry. Fig. 1(a) shows the lowest singlet (1A) and triplet CTTS excited-state (3A) potential energy curves taken from the paper of Villa and Jordan [19]. Notice that the active space employed in their calculations was quite small (two electrons were distributed in two orbitals) and the basis set used was also small. In order to confirm the accuracy of their CASPT2 calculations, we have further carried out additional CASPT2 calculations. Eight electrons were distributed among the I-5 sp orbitals the dipole-bound orbital. For water, the 6-31(1+,3+)G* basis set was used and the SDD effective core basis set augmented by diffuse s and p as well as polarization d and f functions [20] was used for an I atom. The result of this CASPT2 calculation was plotted in Fig. 1(b). It is seen that agreement between the result of Villa and Jordan and the present result is reasonably good. Fig. 1(c) shows the potential energy curve obtained from the present triplet B3LYP calculations. Note that only the relative energies are plotted with the local minima being set to zero. It is seen from Fig. 1 that the singlet CASPT2 potential curve almost coincides with the triplet potential curve, implying that the singlet-triplet splitting is quite small. It is also noticed that the triplet B3LYP potential curve is quite similar to the CASPT2 curves; all curves show minima at ~ 125 degrees of the dihedral angle. It should be emphasized that these minima cannot be seen in the CASSCF results (not shown, see Fig. 4 of Ref. 19). This is quite encouraging that the B3LYP potential is similar to the CASPT2 result rather than the CASSCF result. Notice that the previous direct dynamics calculations for the $\Gamma(\text{H}_2\text{O})_3$ cluster were carried out on the

CASSCF potential energy surface. This tentatively suggests that the dynamics calculations on the B3LYP potential surface may be more reliable than those on the CASSCF potential surface.

It should also be important to confirm small singlet-triplet energy splittings for the $\Gamma(\text{H}_2\text{O})_6$ cluster, since actual dynamics calculations will be done for this cluster. We have carried out single-point calculations for the optimized Bf-type $\Gamma(\text{H}_2\text{O})_6$ structure at the CASPT2 level of theory with the 6-31(1+,3+)G* + SDD basis set. Eight electrons were distributed among the I-5*sp* orbitals the dipole-bound orbital. Notice that the chosen active space was much larger than that used in the theoretical work of Villa and Jordan [19]. As a result, it was found that the lowest triplet state is slightly stable than the lowest singlet excited state similar to the $\Gamma(\text{H}_2\text{O})_4$ case and that the corresponding splitting is only 0.028 eV. If we add the diffuse *s* and *p* and as well as polarization *d* and *f* functions [20] to the I-SDD basis set, the splitting energy was calculated to be somewhat large (0.054 eV) but this value is again quite small. All these results suggest that the triplet surface is the proper choice for the $\Gamma(\text{H}_2\text{O})_6$ dynamics.

3. Results and discussion

Fig. 2 shows the time evolution of the total kinetic energy, total electronic energy (potential energy), dipole moment, and vertical electron detachment energy (VDE) for the photoexcited Bd $\Gamma(\text{H}_2\text{O})_6$ cluster. The dipole moment was obtained from the same level B3LYP calculations of the doublet neutral state for the geometry at each time step. The VDE values were also determined from this neutral state calculation. The corresponding structural change is shown in Fig. 3 along with the change of electron density of the highest occupied molecular orbital (HOMO). Just after photoexcitation, the "dangling" hydrogen atoms, which initially support the Γ atom in the ground state, move away from the I atom within 23 fs. This initial process is accompanied by a sudden drop in the potential energy and by a sudden rise in kinetic energy. After this, hydrogen atoms keep moving and deformation of the book-type structure, constructed from the six oxygen atoms, is seen up to t

~ 801 fs although the book-type structure is maintained. It is interesting to note that the average potential energy value gradually decreases up to $t \sim 800$ - 900 fs. The most interesting feature, which can be seen from Fig. 3, is that the I atom initially and slowly departs from the water cluster, but that the I atom comes back to the water cluster. At $t = 801$ fs, it is clearly seen that the I atom attached to the oxygen atom of one of the six water molecules. This is an expected result; however, it is not surprising because of the attractive interaction between I and H_2O in the ground electronic state. Kowal et al. [21] have previously studied the binding energy between I and H_2O using a sophisticated ab initio electronic structure method. Their CCSD(T) calculation gives the I-OH₂ binding energy to be 1.9 kcal/mol. We have also estimated the I-OH₂ binding energy with the present B3LYP/6-31(1+,3+)G* level and a somewhat larger binding energy of 4.7 kcal/mol was obtained. Although the B3LYP value may presumably be too large, the present trajectory simulation suggests the importance of the attractive interaction between the neutral I atom and water molecules.

It is seen that the book-type structure, i.e., one hydrogen bond, is broken at $t \sim 900$ fs and after this, it is interesting to note the potential energy gradually increases. This result qualitatively suggests that the structural change in the time range of $0 \leq t \leq 900$ fs is controlled by the feature of the potential energy surface. In other words, the structural change occurs along the direction of the potential energy decrease. However, since a relatively large energy is already partitioned into the atomic kinetic energy of the system, a statistical behavior may play a more important role in the trajectory for $t > \sim 900$ fs.

Another feature of the relaxation dynamics of photoexcited Bd-type I(H_2O)₆ clusters is that the dipole moments as well as VDE values are relatively small in this time range although slight increases is seen at $t \sim 800$ - 900 fs. This behavior is also seen in the excess electron density plot presented in Fig. 3. It can be seen that the location of the excess electron is strongly dependent on the cluster structure. The excess electron is mainly distributed around the dangling hydrogen atoms but the positions of the dangling H atoms frequently change along the trajectory.

Totally different pictures were obtained in the relaxation dynamics of photoexcited Bf-type I(H_2O)₆ clusters. Fig. 4 shows the similar plot as Fig. 2 but for the Bf initial

structure. The corresponding structural change as well as the excess electron density change are shown in Fig. 5 along this trajectory. It is interesting to notice that the excess electron is initially distributed around the one dangling hydrogen in the H_2O molecule, whose the other hydrogen atom supports the I atom. It is seen that the excess electron is always distributed around the same position at all along this trajectory. Both the dipole moments and VDE values are much larger than those for the Bd trajectory result. In particular, it is found that the dipole moment gradually increases with the increase in time. At this point, it should be important to comment on recent theoretical calculations by Herbert and Head-Gordon [16,17]. They have carried out systematic VDE calculations for $(\text{H}_2\text{O})_n^-$ cluster anions, as mentioned previously, and concluded that the B3LYP level calculation generally gives large VDE values. Thus, it is possible that the present B3LYP/6-31(1+,3+)G* calculation yields too large VDE values for the $\Gamma(\text{H}_2\text{O})_n$ systems. It may be somewhat unrealistic to compare the absolute values of VDE at the B3LYP/6-31(1+,3+)G* level with experimental excess electron binding energies.

The average value of the potential energy decreases up to $t = 500$ fs and the book-type structure is kept in this initial process. It is also interesting to notice the increase in the VDE values around $t = 500$ fs. Once a large amount of energy is partitioned into the atomic kinetic energy, the break of hydrogen bonds is seen to occur. In this trajectory, it is seen that a linear type $\Gamma(\text{H}_2\text{O})_6$ cluster is finally produced. Also, similar to the Bd trajectory case, the I atom does not detach from the water cluster.

Although a large number of trajectories, starting from many different initial configurations as well as different initial kinetic energy distributions, should be done in order to make a concrete connection with the experimental results, our limited simulation qualitatively suggests that the VDE shift observed in the femtosecond experiments [2-4] can be partly explained by the relaxation dynamics of the photoexcited Bf-type $\Gamma(\text{H}_2\text{O})_6$ cluster. According to the previous theoretical calculations [18] as well as the present B3LYP level calculations, the Bd-type $\Gamma(\text{H}_2\text{O})_6$ cluster in the ground state is slightly more stable than the Bf-type cluster. When the Bd-type $\Gamma(\text{H}_2\text{O})_6$ cluster is photoexcited, a simple population decay is presumably the most probable channel since both the VDE value and dipole moment are significantly small. Another important conclusion derived from the present simulation is

the I atom detachment was not observed. However, this does not mean that the I atom dynamics is not important in the relaxation dynamics. In fact, in the early stage of the trajectory ($0 \leq t \leq 431$ fs) presented in Fig. 5, it is seen that the I atom moves away from the excess electron distribution and this process may cause the change in the excess electron distribution. In this regard, the present simulation shows that the iodine motion also plays some roles in determining the time-evolution of the excess electron binding energy following photoexcitation. It is possible that the neutral iodine atom cannot be detached from the system due to the overestimated binding energy between I and water molecules. The time-resolved experiments of Kammrath et al.[4] implied that I atom loss occurs prior to autodetachment; however, they have concluded that the I atom loss occurs at very long times ~ 38 ps. Notice that this quite long time is beyond the present simulations.

In summary, we have carried out direct dynamics simulations of the photoexcitation of the $\text{I}(\text{H}_2\text{O})_6$ cluster anion for the first time. We analyzed the time evolutions of electronic properties along the classical trajectory on the CTTS excited-state potential energy surface. Although our simulations were done with very limited initial conditions, we were able to obtain a reasonable theoretical picture that can qualitatively explain the pump-probe femtosecond photoelectron experiments of Neumark and co-workers [2-4]. In the near future, we will report results of direct dynamics calculations for other initial configurations since several other conformers have previously been found. In addition, we will extend the present simulations to $\text{I}(\text{H}_2\text{O})_n$ cluster anions with different sizes. Such studies are currently in progress in our laboratory.

References

- [1] D. Serxner, C. E. H. Dessent, M. A. Johnson, *J. Chem. Phys.* 105 (1996) 7231.
- [2] L. Lehr, M. T. Zanni, C. Frischkorn, R. Weinkauff, D. M. Neumark, *Science* 284 (1999) 635.
- [3] A. V. Davis, M. T. Zanni, R. Weinkauff, D. M. Neumark, *Chem. Phys. Lett.* 353 (2002) 455.
- [4] A. Kammrath, J. R. R. Verlet, A. E. Bragg, G. B. Griffin, D. M. Neumark, *J. Phys. Chem. A* 109 (2005) 11475.
- [5] J. R. R. Verlet, A. Kammrath, G. Griffin, D. M. Neumark, *J. Chem. Phys.* 123 (2005) 231102.
- [6] D. E. Szpunar, K. E. Kautzman, A. E. Faulhaber, D. M. Neumark, *J. Chem. Phys.* 124 (2006) 054318.
- [7] H.-Y. Chen, W.-S. Sheu, *Chem. Phys. Lett.* 335 (2001) 475.
- [8] H.-Y. Chen, W.-S. Sheu, *Chem. Phys. Lett.* 353 (2002) 459.
- [9] H. M. Lee, S. B. Suh, K. S. Kim, *J. Chem. Phys.* 119 (2003) 7685.
- [10] Q. K. Timerghazin, G. H. Peslherbe, *J. Am. Chem. Soc.* 125 (2003) 9904.
- [11] M. Kołaski, H. M. Lee, C. Pak, M. Dupuis, K. S. Kim, *J. Phys. Chem. A* 109 (2005) 9419.
- [12] A. D. Becke, *J. Chem. Phys.* 98 (1993) 5648.
- [13] T. Takayanagi, *J. Phys. Chem. A* 110 (2006) 7011.
- [14] Gaussian 03, Revision B.04, M. J. Frisch et. al, Gaussian, Inc., Pittsburgh PA, 2003.
- [15] A. Bergner, M. Dolg, W. Kuechle, H. Stoll, H. Preuss, *Mol. Phys.* 80 (1993) 1431
- [16] J. M. Herbert, M. Head-Gordon, *J. Phys. Chem. A* 109 (2005) 5217.
- [17] J. M. Herbert, M. Head-Gordon, *Phys. Chem. Chem. Phys.* 8 (2006) 68.
- [18] H. M. Lee, K. S. Kim, *J. Chem. Phys.* 114 (2001) 4461.
- [19] F. D. Villa, K. D. Jordan, *J. Phys. Chem. A* 106 (2002) 1391.
- [20] M. N. Glukhovtsev, A. Pross, M. P. McGrath, L. J. Radom, *J. Chem. Phys.* 103 (1995) 1878.
- [21] M. Kowal, R. W. Gora, S. Roszak, J. Leszczynski, *J. Chem. Phys.* 115 (2001) 9260.

Figure Captions

Fig. 1 Potential energy curves for the $\Gamma(\text{H}_2\text{O})_4$ cluster as a function of the dihedral angle (see text for detail): (a) CASPT2 results taken from Ref. 19, (b) present CASPT2 results (see text) and (c) B3LYP result.

Fig. 2 Time evolutions of the total kinetic energy (a), total electronic energy (b), dipole moment (c), and vertical detachment energy (d) along the trajectory of the photoexcited Bd-type $\Gamma(\text{H}_2\text{O})_6$ cluster.

Fig. 3 Snapshots of selected configurations along the trajectory of the photoexcited Bd-type $\Gamma(\text{H}_2\text{O})_6$ cluster. The O-H hydrogen bonds and I-H bonds are drawn using dotted lines and dashed lines, respectively. The corresponding excess electron density plots are also shown.

Fig. 4 Same as Fig. 2 but for the Bf-type cluster.

Fig. 5 Same as Fig. 3 but for the Bf-type cluster.

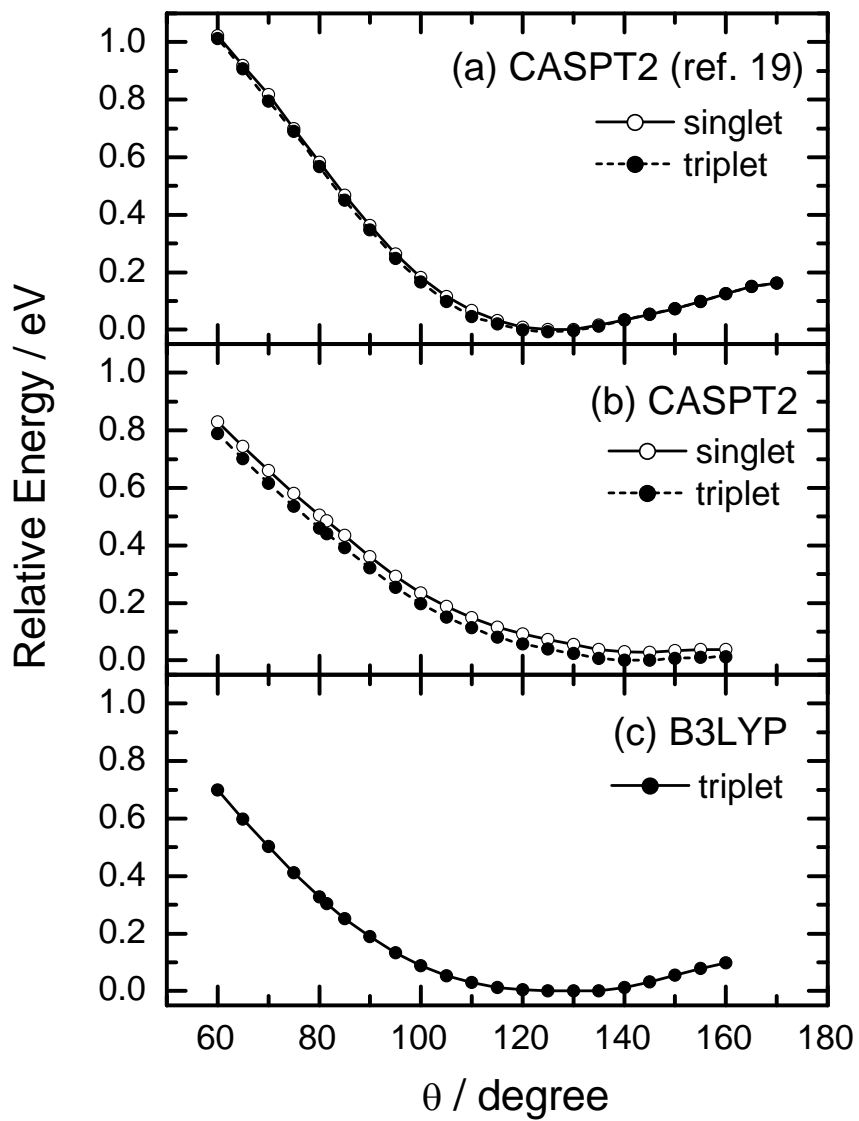
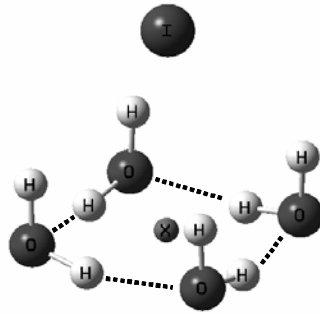


Figure 1

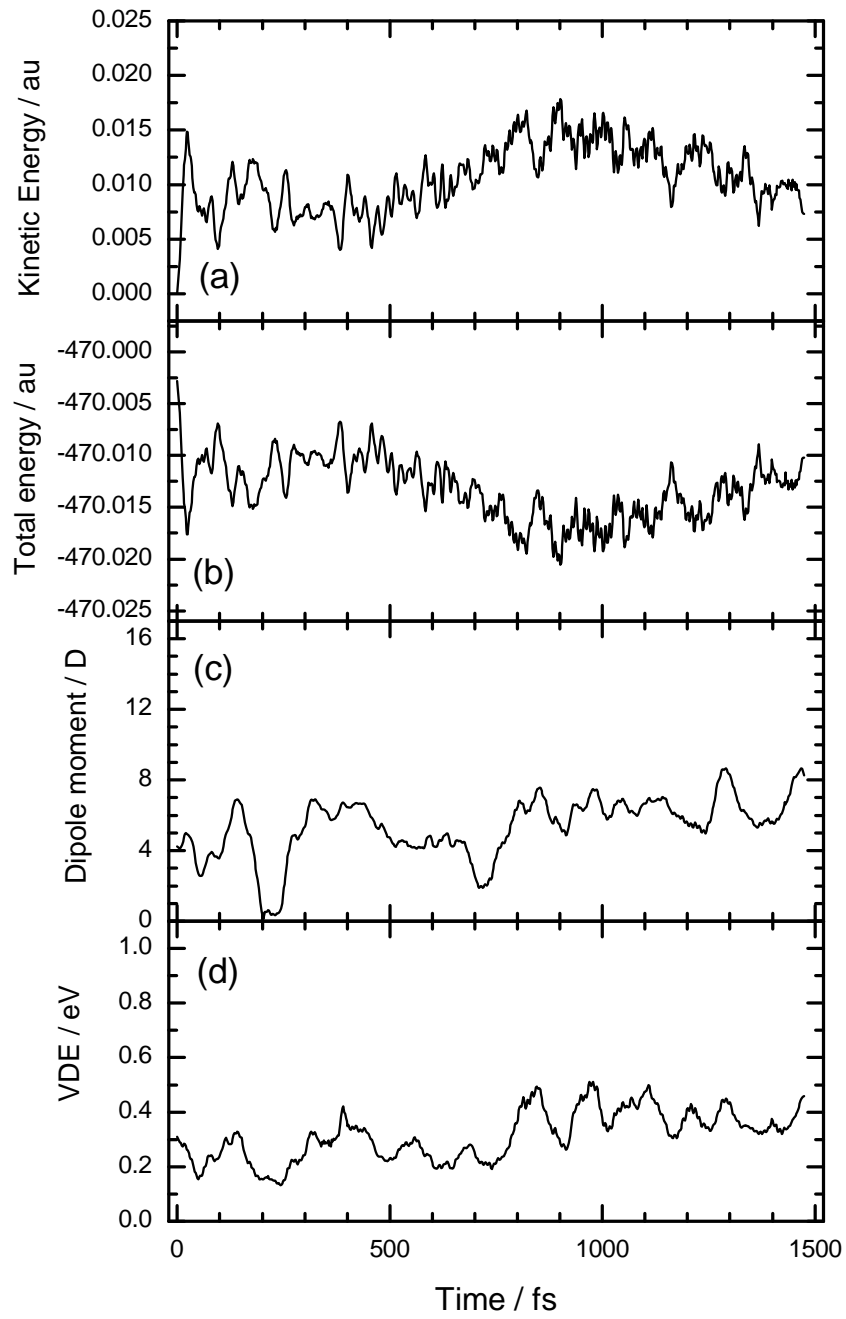


Figure 2

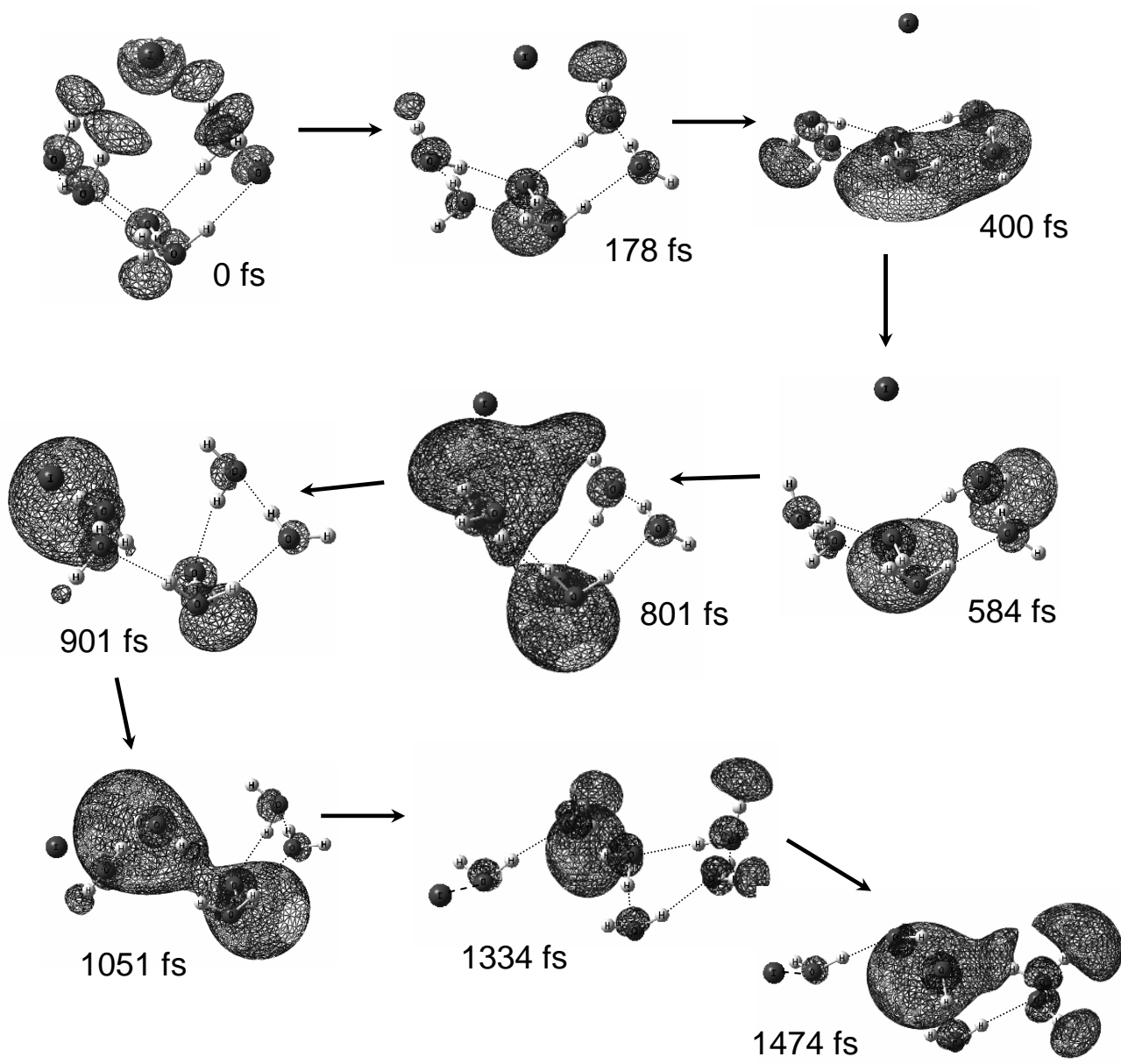


Figure 3

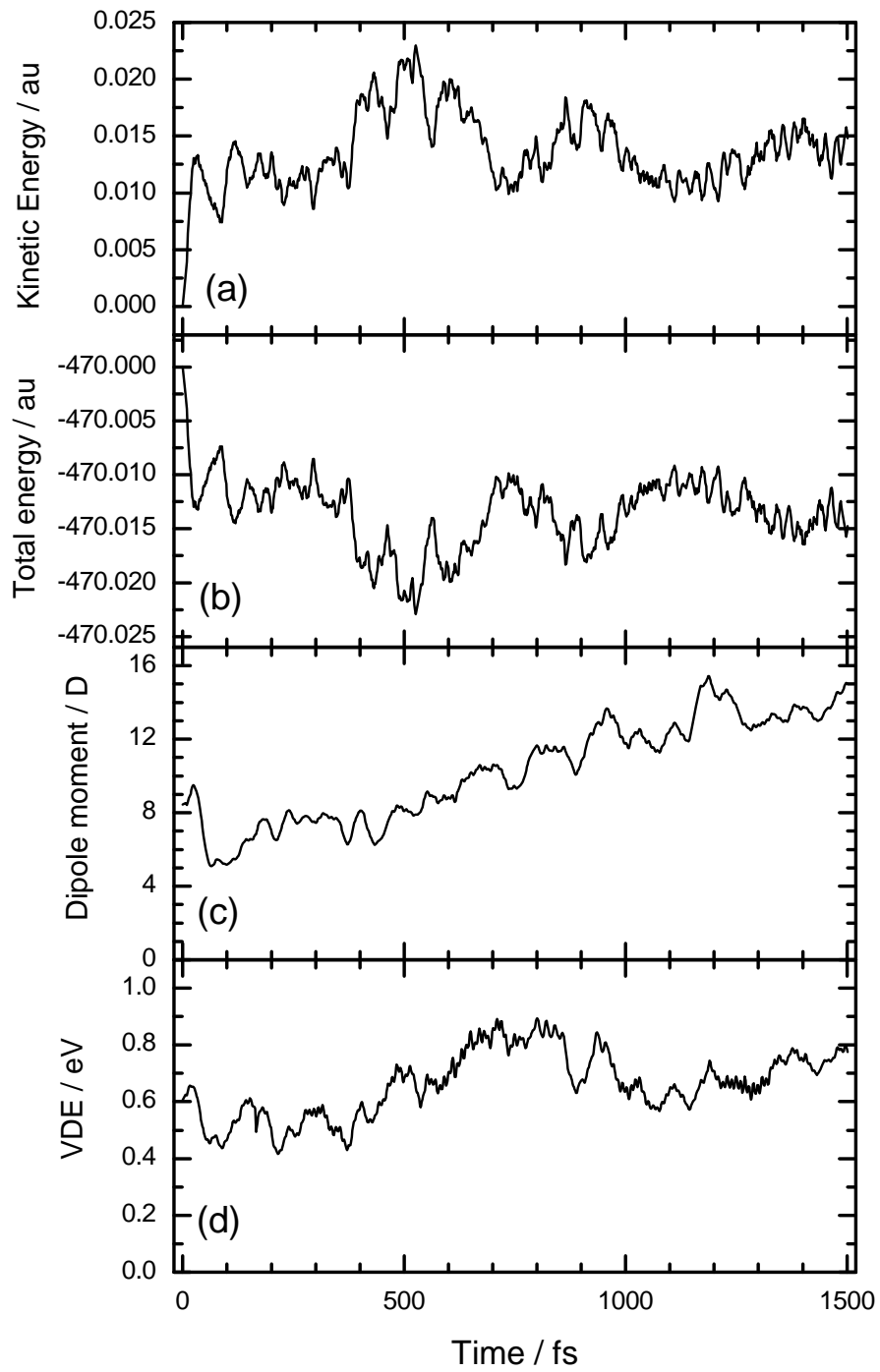


Figure 4

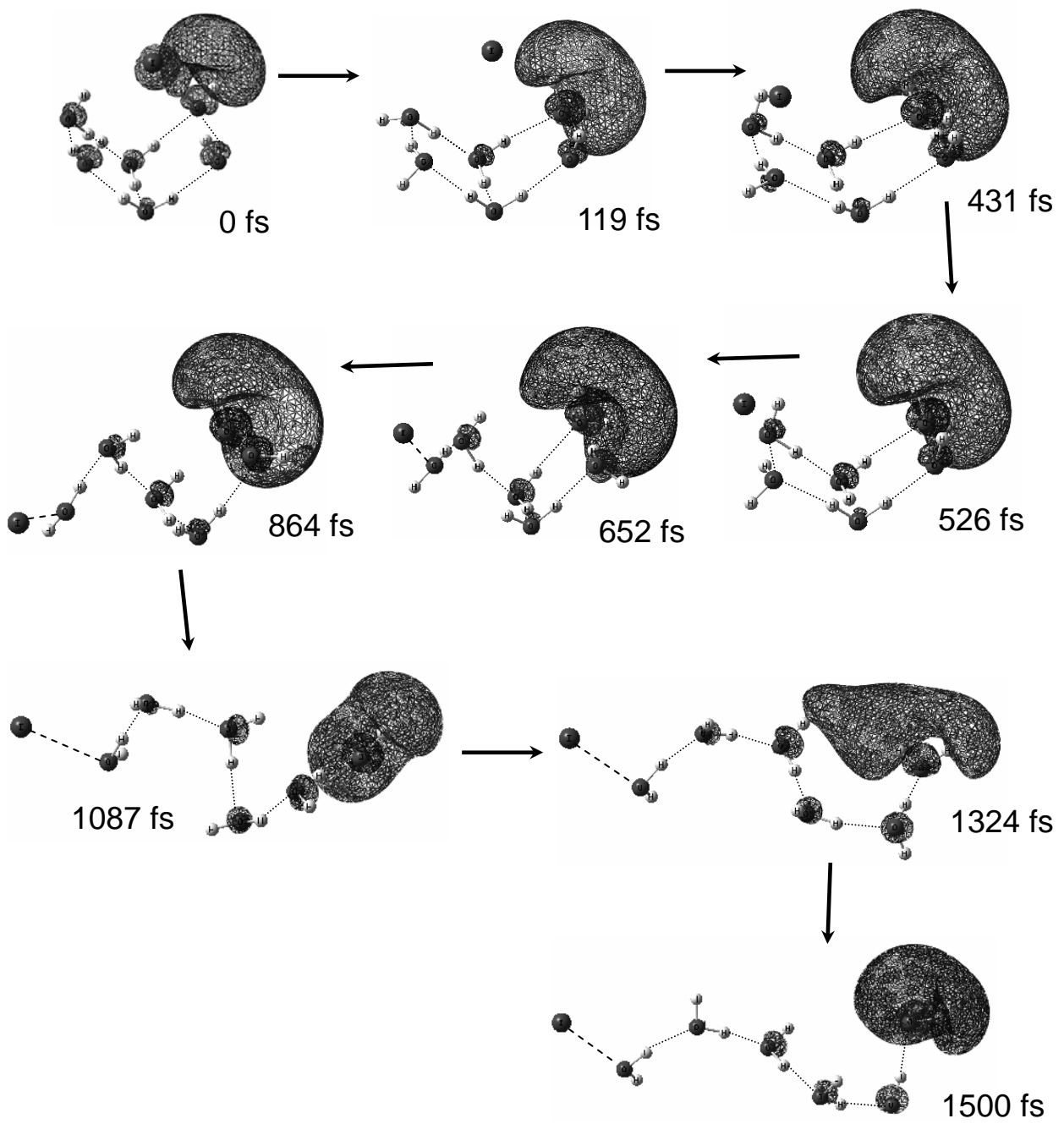


Figure 5